Quarterly Progress Report of the PSI-Center (July - September 2007)

by

Thomas Jarboe, Richard Milroy, Brian Nelson, Uri Shumlak, and Carl Sovinec

The Plasma Science and Innovation Center (PSI-Center) has accomplished a great deal this quarter. The PSI-Center is organized into four groups: Boundary Conditions and Geometry, Two-Fluid and Transport, FLR and Kinetic Effects, and Interfacing. Each group has made good progress and the results from each group are given in detail.

BC&G Group *(U. Shumlak, G. Marklin, W. Lowrie, E. Meier)*

- Finite Element Code Development
    - Incorporated PETSc data structures
    - Incorporated SNES Non-Linear implicit solver framework
        - Used analytic function and Jacobian calculations
        - Added SuperLU for linear system direct solves
        - Added KSP (Krylov Subspace) for iterative linear solves
    - Added ability of code to handle higher-order (hp) elements
        - Variable order Lagrange basis functions
        - Legendre-Gauss quadrature for definite integrals
    - Generalized code to handle generic flux and source terms for easier equation and boundary specification (i.e. f(q) and f(q'))
    - Modularized code such that the solver and physics specification are completely separate, which enables easy physics equation defining.
    - Added framework for top level boundary condition specification
- Ported SEL Code to PSI computer system.
- Implicit induction equation advance in MH4D is now compatible with "pie-slice" periodic boundary conditions with or without the periodic axis. Furthermore, matrix preconditioning has been explored and optimized. As a result, computational efficiency is dramatically improved in resistive MHD simulations involving non-parallel periodic boundaries.
- Atomic physics modifications have been implemented in MH4D and tested in spheromak m=1 tilt mode simulations. Total plasma mass increases as background neutral gas is ionized. As expected, the mode growth rate is reduced for the heavier plasma.
- MHD simulations using the insulated conductor boundary condition in the M4 code continue to be plagued by numerical instabilities. Work is currently underway to install a semi-implicit Alfven wave time advance option. This should be sufficient to stabilize the boundary potential equations and will be much less costly then installing a fully implicit time advance - the only alternative.
- The use of mimetic numerical operators is being investigated in the M4 code to assess possible speed and accuracy improvements. A set of numerical operators is called mimetic if preserves curl(grad)=0 and div(curl)=0 as an exact identity. These operators have been shown to significantly improve speed and accuracy in electromagnetic simulation codes where they were developed.

Two-fluid and Transport Group ***(C. R. Sovinec, E. D. Held, R. A. Bayliss, and J.-Y. Ji)***

Over the quarter of funding ending on 9/30/07, the Two-fluid and Transport Group has refined its DC injection computations for HIT-II to use a realistic geometry. We have also developed and tested temperature-dependent parallel viscosity and a new computation for $\mathbf{B}\cdot\nabla T$ that facilitates nonlocal closure computations in the presence of open field-lines. In addition, multiple papers describing moment-based closures are in progress, and a code for assembling collections of rectangular element blocks has been developed.

- Recent NIMROD simulations in a realistic geometry for HIT-II have focused on recovering the MHD fluctuation and relaxation results from the experiment. The mesh is curved from a narrow injector region out through a flux-conserver region and back to a narrow absorber region. Relative to earlier computations in a simplified geometry, poloidal flux tied to the injector region requires more energy to bend out of the narrow opening. Similarly, expanded poloidal flux is less prone to escape from the absorber, because it requires significant field-line bending. In a 0-β computation with S=10^5, B_T ($R_{\min}$)=0.8 T, and injected poloidal flux of 6.5 mWb, the n=1 mode exists throughout the expansion phase, as shown in Fig. TFT.1. The expansion itself temporarily reduces the fluctuation energies, but they increase again after the expansion is complete. Late in time, there is a moderate amount of conversion of toroidal flux to poloidal flux, leading to approximately 40% amplification, but the plasma current does not build with relaxation in this case.

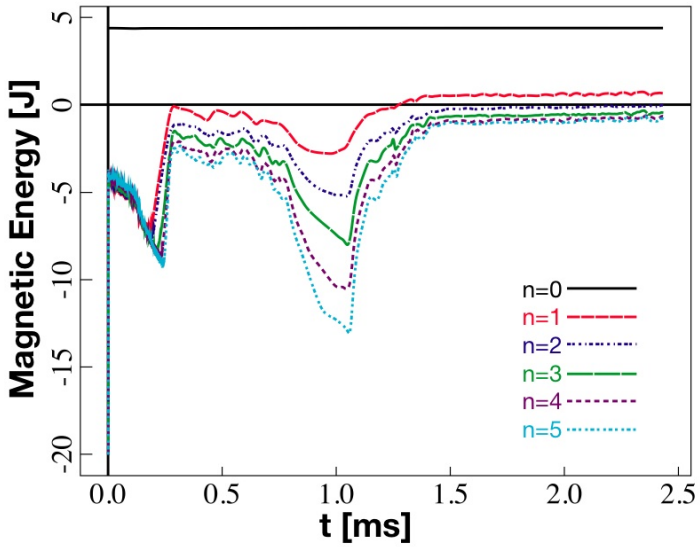

Figure TFT.1. Evolution of magnetic fluctuation energies (logarithm) for the HIT-II simulation.

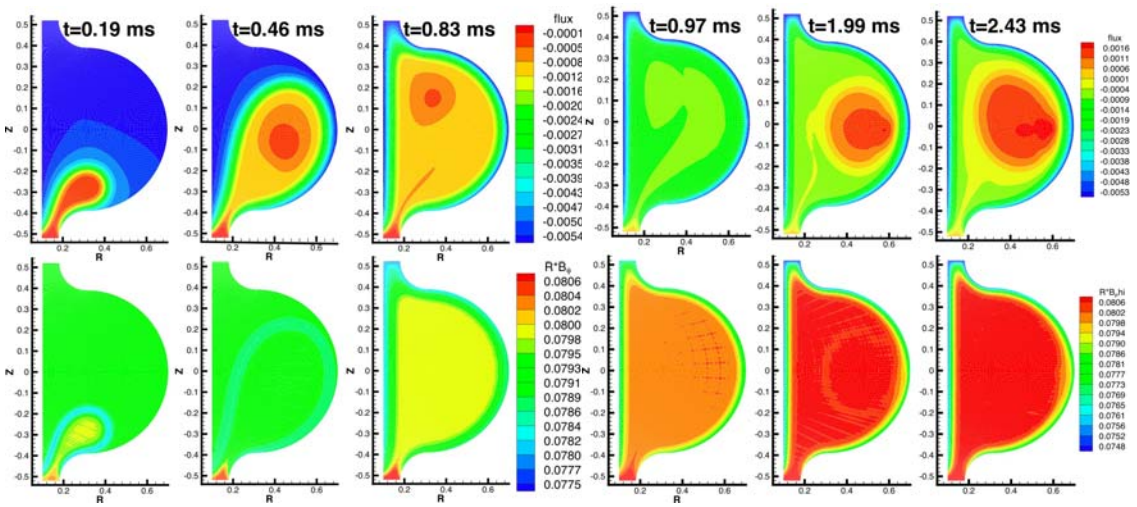

Figure TFT.2. Evolution of poloidal flux (top row) and RB_T contours from the NIMROD simulation of HIT-II. The flux contour scale is changed for the later times to follow the amplification effect.

- We have implemented the general parallel heat flux closure derived from the full moment approach in the NIMROD code and are testing it with the SSPX temperature profile. We are writing a paper that will compare results with Braginskii heat flux and results with the nonlocal closure.
- We have tested the spatial convergence of steady-state temperature distributions in SSPX heat confinement simulations by increasing the polynomial degree of the finite-element basis functions as well as the number of Fourier modes. Two approaches to computing the diffusive (Braginskii), parallel conduction in the temperature equation were explored. The first used the standard formulation, which computes $\hat{\mathbf{b}}\cdot\nabla T$ locally for the right hand side vector using the quadrature point data for **B** and *T*. The other approach finds the projection of $\hat{\mathbf{b}}\cdot\nabla T$ onto the finite-element basis functions via a mass matrix inversion. The quadrature point data from this structure is then used to construct the parallel conduction term. Interestingly, these two methods predicted rather different steady-state *T* distributions with bicubic finite-elements and 6 Fourier components. This is seen in Fig. TFT.3, which shows the temperature profiles for the two approaches when going across the grid in *x* for three values of *y* (mesh coordinates). For the profile going directly through the core (the two profiles with the highest temperature), the one that peaks around 107 eV is that associated with the mass-matrix inversion approach, whereas the cooler profile through the core (peaking around 74 eV) is from the standard NIMROD calculation of anisotropic conduction. Relatively well-converged computations, which use biquartic elements and 22 Fourier modes, are shown in Fig. TFT.4 for the same slice locations. One important observation is that the under-resolved mass matrix inversion case appears to be closer to the final converged solution, suggesting that it is a more accurate means of computing the diffusive parallel heat flow closure. These results also suggest that for quantitative computation of heat transport along stochastic fields, a significant amount of resolution is required in the periodic direction. Since the temperature substantially influences resistivity and conductivities, the need for enhanced resolution in turn affects the magnetic evolution in integrated MHD/transport simulations.

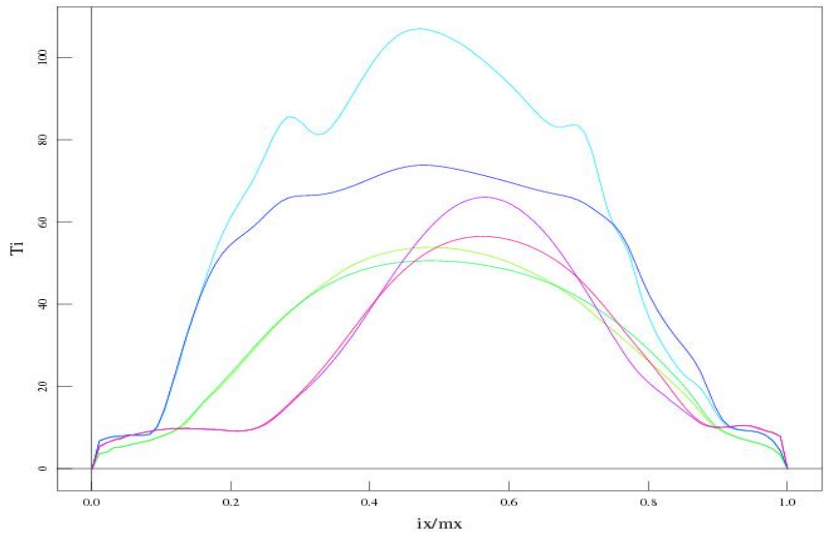

Figure TFT.3. Low-resolution (bicubic elements and $0 \le n \le 5$) results from heat-flow calculations using the geometry and 3D magnetic field from an SSPX simulation with NIMROD. Three separate slices are shown for each computation, and the two calculations differ in their computation of $\hat{\mathbf{b}} \cdot \nabla T$.

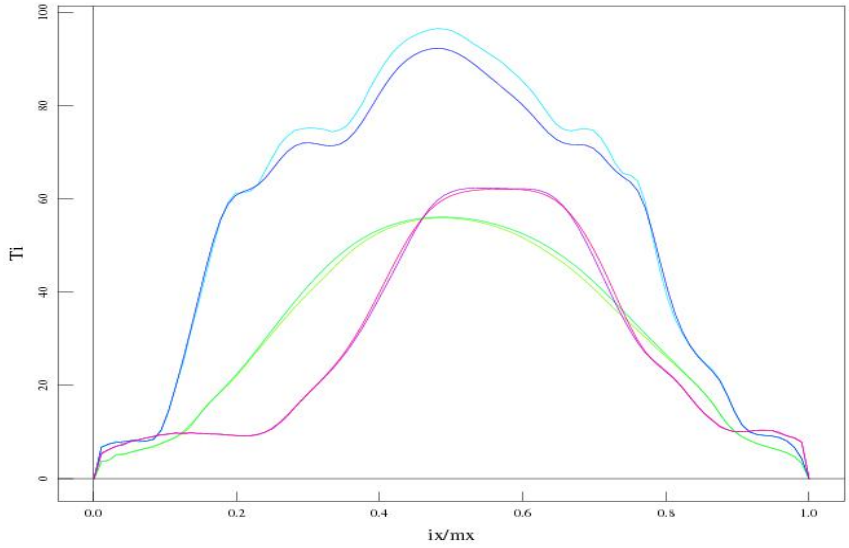

Figure TFT.4. Results from heat-flux calculations with biquartic elements and $0 \le n \le 21$.

- Analytically, we have derived general moment equations and collision operators for two-fluid plasmas based on the random-velocity expansion of the distribution functions. A paper describing this work is nearly complete. We have also derived the classical (Braginskii) closures from the general moment equations and found additional terms for the Braginskii equations. A paper describing this work is also being written.
- Coding for temperature dependence in the Braginskii ion parallel stress computation, $\Pi_{||} = (p_i \tau_i / 2)\left(\hat{\mathbf{b}} \cdot \mathbf{W} \cdot \hat{\mathbf{b}}\right)\left(\mathbf{I} - 3\hat{\mathbf{b}}\hat{\mathbf{b}}\right)$, where $\mathbf{W}$ is the traceless rate-of-strain tensor, has been implemented and tested in NIMROD. The coefficient is computed locally and is used in a 'matrix-free' implicit advance of velocity in three-dimensional simulations. The toroidal average of the coefficient is used in preconditioning the velocity-field solves. Our quantitative tests check viscous damping in compressive low-frequency waves. In

conditions of weak damping ($k^2\nu << \omega$, where $\nu = k_B T_i \tau_i / m_i$), simple dispersion-relation analysis shows that the expected damping rates for the perpendicular magnetoacoustic wave and the parallel ion sound wave are $\nu k^2/6$ and $2\nu k^2/3$, respectively. The Alfven wave is not damped. Numerical tests of the new nimrod algorithm with $\omega\Delta t$ = 0.2-0.3 are provided in the table below. Also, the presence of parallel viscosity does not damp Alfven waves, as expected.

Damping results (ν/ω) from NIMROD computations with T-dependent parallel viscous stress.

Wave	T_i=1		T_i=0.5	
	analytical	computed	analytical	computed
Magneto-acoustic	0.0106	0.0103	0.00193	0.00177
Ion sound wave	0.0595	0.0581	0.00106	0.00104

- Though it is somewhat outside the focus of the Two-fluid and Transport Group, we have developed a new driver program, 'stitch,' for assembling regions of rblocks (logically rectangular blocks of quadrilateral elements) into irregular arrangements. A very simple example is shown in Figure TFT.5, and much more complicated arrangements are possible. The program replaces nimset as the driver for pre-processing, and the user generates separate regions using unmodified nimset routines and then interactively instructs the program how to stitch these regions together. The program then modifies the seam information that is used to tell nimrod how grid blocks are connected to each other. Stitching operations are allowed to produce non-conforming connections among blocks, as long as elements are left with compatible neighboring elements. The first production application is for the design of a modification to the SSPX spheromak experiment.

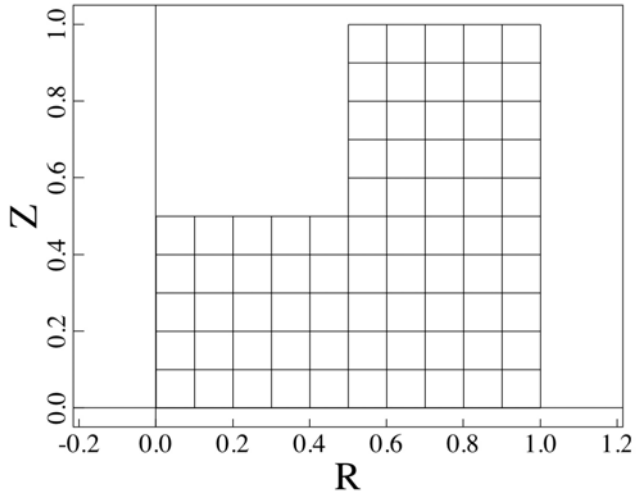

Figure TFT.5. Example of a mesh created by stitching. The region defined for $0 \le x \le 0.5$, $0 \le y \le 0.5$ has one grid block and is stitched to another region for $0.5 \le x \le 1$, $0 \le y \le 1$ that also has one grid block.

FLR and Kinetic Effects Group *(R. Milroy, A. Macnab, C. Kim)*

During this quarter, Charlson has devoted most of his time to the interface group, and Angus has recently left the Ψ-Center.

Accomplishments

- We have completed the task of compiling a serial version of NIMROD on the Windows platform. This is an attractive platform for those familiar with Visual Studio, since it incorporates a fast and powerful debugger. We are using the Intel FORTRAN 10.0.26 along with the Microsoft Visual C++ 2005 to compile the C components including SuperLU.

- Progress has been made in developing end boundary conditions that are more suitable for FRC simulations. We now have options to initialize FRC simulations with an initial low density and pressure at the boundaries, and to maintain this low density with a Dirichlet boundary condition along with a highly shaped particle diffusivity near the boundary.

- Work has begun to allow for simulations of Rotating Magnetic Field (RMF) current drive in FRCs. To begin, we are applying a rather simple RMF boundary condition corresponding to a rotating but axially uniform n=1 component of B_r and a corresponding axially uniform n=1 component to E_z. A new FORTRAN RMF MODULE was developed in NIMROD to implement RMF in a modular and object oriented manner. Numerical problems are being encountered after significant velocities are induced and the *density floor algorithm kicks in*. However, this is after significant penetration and current drive is evident, as illustrated in figure.

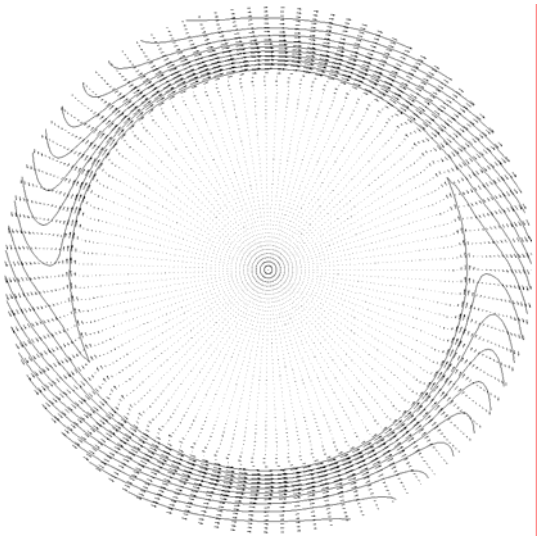

Magnetic field vectors superimposed on the n=1 "field-lines" illustrating RMF penetration in a NIMROD simulation.

- Little progress was made with the n=2 rotational instability study, as it was put on the *back-burner* for most of this quarter. We hope to resume work on this topic during the next quarter, and report results at the upcoming APS meeting.

- We have been studying the drift-kinetic tokamak (1,1) kink mode simulations to help understand the mechanism for the FLR stabilization of the RFP tearing mode.

Interfacing Group *(B. A. Nelson, C. C. Kim, A. Cassidy, S. D. Griffith)*

Accomplishments

- The IG is tasked with assisting in computational support for the twelve collaborating ICC experiments (along with the three physics groups). All collaborating PIs have been contacted, and development of plans for proceeding with simulations is ongoing.
- Work is continuing on the Levitated Dipole Experiment (LDX).
    - Improved gridding for the LDX geometry to align finite elements along pressure contours. Also the aligned grid is packed proportional to pressure, improving computational efficiency by factor of 2-4.
    - Added Gaussian profile density and heat source terms to NIMROD equations and ran LDX simulations to generate suitable equilibria for interchange studies.
    - Preliminary nonlinear simulations (with low *n* mode numbers) with and without source terms do not indicate any instability. This may be due to relatively high viscosity and/or resistivity.
    - Added a subroutine to transfer *n*=0 fields to *_eq variables to allow linear simulations.
    - Preliminary simulations show some mode growth but results are questionable due to high divb errors and location of mode peaking.
- Work is continuing with assisting UW graduate student Cihan Ackay with HIT-SI simulations, including compilation, meshing, importing equilibria, and conversion to the most current version of NIMROD. Nonlinear simulations of poloidal flux amplification show good agreement with previous (V. Izzo) simulations.
- Progress is continuing on the NimPy post-processor, which outputs NIMROD data to the Visualization Toolkit (VTK) format, which can then be read by the LLNL VisIt visualization program (http://www.llnl.gov/visit/). Code cleanup, and command line improvements have been implemented.
- Dr. Kim is working with Dr. Scott Kruger of TechX to merge NIMlite (PSI-Center version) with NIMdevel (TechX version). NIMlite removes vestigial elements of old coding and includes reorganization of the code for more efficient compilation.